D22

22

APPLICATION OF THE AMI $C_{\ell_{max}}$ PREDICTION METHOD TO A NUMBER OF AIRFOILS*

F.A. Dvorak and B. Maskew
Analytical Methods, Inc.

SUMMARY

A method for calculating the flow about airfoils up to and beyond the stall is described. It is an iterative procedure between potential flow and boundary layer solutions. The separated region is modeled in the potential flow analysis using free vortex sheets which require an inner iteration to establish their shapes. The free vortex sheet length is an important parameter in the potential flow calculation. Results so far indicate a possible correlation between wake length and airfoil thickness/chord ratio. Calculated and experimental results are compared for a series of airfoils.

INTRODUCTION

Boundary layer separation is one of the least understood but most important of fluid flow phenomena affecting aerodynamic forces and moments. Its accurate modeling is essential to the estimation of airborne vehicle performance. Currently, reliance is placed on wind tunnel tests to determine the consequences of separation, a procedure which is not entirely free of doubt because of Reynolds number effects. Successful theoretical modeling of separation is limited to a small number of special cases, one of which is two-dimensional turbulent boundary layer separation from airfoils or diffusers. The first successful model for trailing-edge separation was developed by Jacob (ref. 1). With Jacob's model, the separation region is simulated using source fluid, the distribution of which is chosen to give constant pressure everywhere in the separation region. In general, the method predicts the upstream pressure distribution in a satisfactory manner, although agreement with experiment for base pressure level is not consistent.

Recently a separation model has been developed by Analytical Methods, Inc. which replaces the source distribution in the separation zone by a vortex wake model. This model is described in

*Support was given by the U.S. Army Research Office, Research Triangle Park, N.C., for this work under Contract DAAG29-76-C-0019.

346

some detail in reference 2, but is discussed herein for reasons of completeness.

Symbols are defined in an appendix.

SEPARATION MODEL

Approximations for the Complete Flow Field

An approximate model of the flow about an airfoil with a region of separation is shown in figure 1. It is assumed that:

(i) The boundary layer and free shear layers do not have significant thickness and, hence, can be represented as slip surfaces; that is, streamlines across which there exists a jump in velocity.

(ii) The wake region does not have significant vorticity and has constant total pressure (lower than the free-stream total pressure). It is, therefore, taken to be a potential flow region.

The flow field in the potential flow is obtained using linearly varying vortex singularities distributed on planar panels. The wake is represented by sheets of vorticity shed at the separation points.

The mathematical problem is to find the vorticity sheet strength such that the appropriate boundary conditions are met. The position of the vorticity sheet representing the free shear layer is not known a priori.

Approximations For the Free Shear Layer

(i) Wake Shape

Initially, the streamlines are not known, and so the shapes of the free shear layers must be obtained iteratively starting from an initial assumption. Earlier calculations in which the vortex sheet shapes were obtained by iteration suggested an initial shape as follows. The upper and lower sheets are represented by parabolic curves passing from the separation points to a common point downstream. The slope at the upstream end is the mean between the free stream direction and the local surface slope. (Indications from further calculations are that this starting slope should be streamwise for calculations beyond the stall.) Once the wake calculation begins, the initial slope and downstream position of each wake is determined by iteration. The final wake position represents the separating streamline.

(ii) Wake Length

Early calculations indicated that the results were sensitive to the length of the free vortex sheets. Good correlation with experimental results was obtained only with relatively short wakes, i.e., wakes extending .1c to .2c beyond the trailing-edge. Such a model appears reasonable in the light of experimental evidence: the separated wake does, in fact, close quickly downstream of the trailing-edge, as a result of the strong entrainment process brought about by the rotation in the free shear layers (see reference 3). On the basis of several comparisons with experiment, a simple correlation was obtained for the wake length as a function of the airfoil thickness to chord ratio. This is discussed in detail in reference 2.

(iii) Wake Pressure

The approximation of zero static pressure drop across the free shear layer is used to obtain an expression for the total pressure in the wake in terms of the strength of the free vortex sheets. Considering the upper shear layer, if the average velocity in the layer is denoted by

$$\bar{V} = \tfrac{1}{2}\left(V_{outer} + V_{inner}\right)$$

then

$$V_{outer} = \bar{V} + \gamma_U/2, \text{ and}$$

$$V_{inner} = \bar{V} - \gamma_U/2,$$

since the vorticity, $\gamma_U = V_{outer} - V_{inner}$, on the upper sheet. (The vorticity in the lower shear layer is $\gamma_L = V_{inner} - V_{outer}$.) The jump in total pressure across the shear layer is then

$$\begin{aligned}\Delta H &= H_{inner} - H_{outer} \\ &= \left\{p_{inner} + \tfrac{1}{2}\rho\left(\bar{V} - \gamma_U/2\right)^2\right\} \\ &\quad - \left\{p_{outer} = \tfrac{1}{2}\rho\left(\bar{V} + \gamma_U/2\right)^2\right\} \\ &= -\rho\bar{V}\gamma_U = \rho\bar{V}\gamma_L\end{aligned}$$

given the boundary condition that the static pressure, p, has no jump in value across the shear layer.

Since the wake has constant total pressure (assumption (ii)), the jump in total pressure across the free shear layer is the same everywhere.

Once the vorticity strengths of the individual panels representing the airfoil and of the vorticity sheets representing the wake are determined, the velocity at any point in the flow field can be calculated.

The pressures are calculated from the velocities according to the Bernoulli equation which is expressed non-dimensionally as

$$C_p = 1 - \left(\frac{V}{V_\infty}\right)^2 + \frac{\Delta H}{q_\infty}$$

where $C_p = \frac{p - p_\infty}{q_\infty}$, $q_\infty = \frac{1}{2}\rho V_\infty^2$, and ΔH = increase in total pressure over that at infinity. Note that $\Delta H = 0$ everywhere except in the wake region for which it was previously shown that $\Delta H = \rho \bar{V} \gamma_L$.

CALCULATION PROCEDURE

Flow-Field Methods

The overall calculation procedure is shown in figure 2, and involves two separate iteration loops.

(i) Wake Shape Iteration

The iteration loop for wake shape is the inner loop and involves the potential flow analysis only. Within this loop the separation points are fixed. The separation points may be located anywhere on a surface panel; they are not restricted to panel edge points.

The wake shape is calculated as follows. Using the previous vorticity distribution, velocities are calculated at the panel mid-points on the free vortex sheets. The new wake shape is then determined by piecewise integration, starting at the separation points. The upper and lower sheet downstream end points, which were coincident in the initial wake, are allowed to move independently in subsequent iterations. At each iteration, the wake influence coefficients at the surface control points are recalculated, and a new potential flow solution is obtained.

The number of wake iterations is an input parameter in the current version of the program; convergence criteria have not been investigated yet.

(ii) Viscous/Potential Flow Iteration

This outer iteration loop takes the potential flow pressure distribution over to the boundary layer analysis and returns with the separation points and with the boundary layer source distribution. The source distribution is determined directly from the boundary layer solution as $\sigma = \frac{d}{ds}(U_e \delta^*)$ where U_e is the streamwise potential flow velocity at the edge of the boundary layer, and δ^* is the displacement thickness. The addition of this source distribution modifies the normal velocity, V_N, at each panel control point. The sources are set to zero in the separated region.

The program generates a new wake shape using the new separation points together with information from the previous iterated wake. A new potential flow solution is then obtained, and so on. The outer iteration is terminated when the change in C_ℓ is below 1%. A limit of eight iterations is currently imposed within the program.

Boundary Layer Methods

The boundary layer development on an arbitrarily-shaped two-dimensional lifting configuration with separated flow is very complex. A thorough and exact calculation of this development is properly the domain of the time-dependent solution to the general Navier Stokes equations. Unfortunately, the computer does not yet exist which is capable of handling such a problem in a reasonable time at a reasonable cost. Such a calculation is not, therefore, of practical interest to the aerodynamicist. Less difficult or costly are the finite-difference boundary layer programs now in existence. The amount of computer time required for each calculation still prohibits their use in an analysis procedure of the type reported herein. Having made the above evaluation, one must conclude that if the objective is a viscosity-dependent calculation procedure of practical use to the aerodynamicist for $C_{\ell_{max}}$ analysis, and, possibly for preliminary design, the method must be relatively simple to use and economic of computer time. This can only be achieved if integral boundary layer methods are used. In two dimensions, integral methods are typically about 100 times faster than finite-difference methods. They can, however, be expected to break down in the region of separation where none of the boundary layer methods (including three-dimensional) can be expected to be valid. It is anticipated, therefore, that integral methods will suffice for most applications of interest to the aerodynamicist for $C_{\ell_{max}}$ prediction.

In those cases of special interest to the aerodynamicist, such as the effect of area suction for boundary layer control or of roughness (rivets, etc.) on $C_{\ell_{max}}$, alternative boundary layer calculation modules are available. These methods are called as needed into the overall calculation procedure. A brief description of the boundary layer methods is given in the following paragraphs.

The laminar boundary layer development is calculated by Curle's method (ref. 4), an adaption of the well known method of Thwaites (ref. 5). The calculation proceeds either to laminar separation or to the end of the airfoil--whichever occurs first. The calculated boundary layer development is then interrogated to determine if transition, laminar separation or forced transition (boundary layer tripping) has taken place. If any of these phenomena have occurred, the downstream flow is assumed to be turbulent.

Methods for the calculation of turbulent boundary layers in two dimensions have been developed by many investigators. A review of these methods was made at a conference held in 1968 at Stanford University (ref. 6). One of the methods, an integral method by Nash and Hicks (ref. 7), compared very favorably with the more complex finite-difference methods. Now, several years later, the method remains an excellent approach for application to the current problem both in terms of accuracy and speed.

If surface roughness or area suction are of interest, an alternate turbulent boundary layer method developed by Dvorak (refs. 8 and 9) can be called. This method is capable of predicting the downstream development and the skin friction drag of a turbulent boundary layer over a rough surface, or a surface with area suction boundary layer control.

Turbulent boundary layer separation is predicted by either the Nash and Hicks or Dvorak methods when the calculated local skin friction coefficient reaches zero.

DISCUSSION OF RESULTS

The method was applied to a GA(W)-1 airfoil. This section shape represents a difficult test case and pressure distributions are available from experiments at NASA-Langley for a range of incidence.

The first set of results, figures 3 through 5, are for a Reynolds number of 6.3×10^6 with a boundary layer trip at .08c. Figure 3 shows a very good agreement between the calculated and

experimental pressure distribution at 20.05° incidence. The calculation took six viscous/potential flow iterations each with three wake shape iterations. For comparison, the attached potential flow solution at this incidence is also plotted, and indicates the large change in pressures due to the separated flow.

The wake shape history for a 21.14° incidence is shown in figure 4, and indicates very good convergence characteristics. Lift and pitching moment characteristics show excellent agreement with experiment, figure 5. The present calculations show considerable improvement over a previous Lockheed/Nasa-Langley calculation. The attached potential flow solution is included in figure 5 to put into perspective the magnitude of the change achieved by the new method.

Figure 6 shows the lift characteristics for the GA(W)-1 airfoil at a Reynolds number of 2.1×10^6. The calculations give good agreement with experiment up to $C_{\ell_{max}}$, but the turnover in the curve occurs 2 to 3 degrees later than in the experiment.

Additional comparisons were made with experiment for several airfoils. Shown on figures 7 and 8 are the results for the lift characteristics for the airfoils tested by McCullough and Gault (ref. 10). In the case of the NACA 63009 airfoil, the program predicts a trailing-edge stall while experimentally the airfoil stalls from the leading-edge. As shown in figure 7, a slight modification to the laminar separation reattachment criterion leads to a much improved correlation with experiment. This points out the need for a better understanding of the laminar separation bubble bursting phenomenon.

Comparisons between theory and experiment for the lift characteristics of the NACA 4412 at a series of Reynolds numbers are shown on figures 9, 10 and 11. A summary of the predicted and experimental $C_{\ell_{max}}$ variation with Reynolds number is shown in figure 12. The calculated values agree very closely with the experimental curve from reference 11. Calculations for lower Reynolds numbers were attempted, but problems with the laminar separation bubble bursting criterion produced inconsistent results.

A series of calculations were made to demonstrate the capability of the analysis method over a wide range of angles-of-attack. Figure 13 shows the calculated wake shape for a NACA 0012 airfoil at 90 degrees to the free stream. The corresponding pressure distribution is given in figure 14. The calculated lift and drag coefficients are 0.25(.15) AND 2.1(2.08 - 2.3) respectively. These values compare well with measured lift and drag coefficients given in the enclosed brackets. Figure 15 shows a

comparison between measured and calculated lift coefficients for the NACA 0012 airfoil from 0 degrees through 90 degrees angle-of-attack. The agreement is surprisingly good.

CONCLUSIONS

The results of comparisons with experiment, including those presented in this paper, lead to the following conclusions

(i) the basic analysis method predicts both the lift curve and the maximum lift coefficient quite accurately for a wide variety of airfoils over a range of Reynolds numbers;

(ii) post-stall behavior is best predicted for the trailing-edge type of stall;

(iii) leading-edge and thin airfoil stall prediction could be considerably improved by a better laminar separation bubble bursting criterion.

(iv) the use of vortex sheets to represent the separated flow boundaries suggests that the model will be applicable to unsteady flows.

APPENDIX

Symbols

c	airfoil chord
C_d	drag coefficient
C_ℓ	lift coefficient
$C_{\ell_{max}}$	maximum lift coefficient
C_m	moment coefficient
C_p	pressure coefficient
H	total pressure
p	static pressure
q	free stream dynamic pressure
Re	Reynolds number, $V_\infty c/\nu$
V_N	normal velocity
$\overline{V}$	average shear layer velocity
V_∞	free-stream velocity
δ^*	displacement thickness
ρ	density
γ	vorticity
σ	boundary layer source strength $\equiv \frac{d}{ds}(V_e \delta^*)$
ν	kinematic viscosity
α	angle-of-attack
U	upper surface

L	lower surface
∞	value at free stream conditions
e	value at edge of boundary layer

REFERENCES

1. Jacob, K., "Computation of Separated, Incompressible Flow Around Airfoils and Determination of Maximum Lift", AVA Report 66, A, 62, 1967.

2. Maskew, B. and Dvorak, F.A., "The Prediction of $C_{\ell max}$ Using a Separated Flow Model", Proceedings 33rd Annual Forum of the American Helicopter Society, Washington, D.C., May 1977. (To be published in the AHS Journal.)

3. Seetharam, H.C. and Wentz, W.H., "Experimental Studies of Flow Separation and Stalling on a Two-Dimensional Airfoil at Low Speeds", NASA CR-2560, 1975.

4. Curle, H., "A Two-Parameter Method for Calculating the Two-Dimensional Incompressible Laminar Boundary Layer", J.R. Aero. Soc., Vol. 71, 1967.

5. Thwaites, B., "Approximate Calculation of the Laminar Boundary Layer", Aero. Quart., Vol. I, 1949.

6. Kline, S.J., Morkovin, M.V., Sovran, G. and Cockrell, D.J., "Computation of Turbulent Boundary Layers", Proceedings 1968 AFOSR-IFP Stanford Conference, Stanford University Press, Stanford, Calif., 1969.

7. Nash, J.F. and Hicks, J.G., "An Integral Method Including the Effect of Upstream History on the Turbulent Shear Stress", Proceedings Computation of Turbulent Boundary Layers--1968 AFOSR-IFP Stanford Conference, Vol. 1, Stanford University Dept. of Mech. Eng., Stanford, Calif.

8. Dvorak, F.A., "The Calculation of Turbulent Boundary Layers on Rough Surfaces in Pressure Gradient", AIAA J., Vol. 7, No. 9, September 1969.

9. Dvorak, F.A., "The Calculation of Compressible Turbulent Boundary Layers with Roughness and Heat Transfer", AIAA J., Vol. 10, No. 11, November 1972.

10. McCullough, G.B. and Gault, D.E., "Examples of Three Representative Types of Airfoil Section Stall at Low Speed", NACA Tech. Note 2502, 1951.

11. Pinkerton, R.N., "The Variation with Reynolds Number of Pressure Distribution over an Airfoil Section", NACA Report No. 613, 1938.

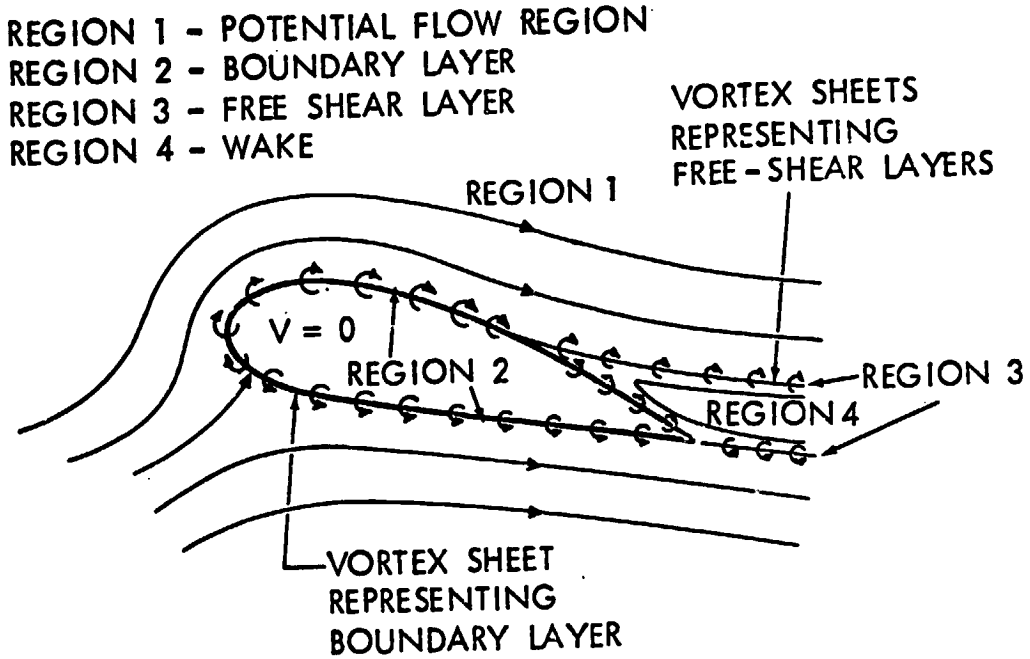

Figure 1.- Mathematical flow model.

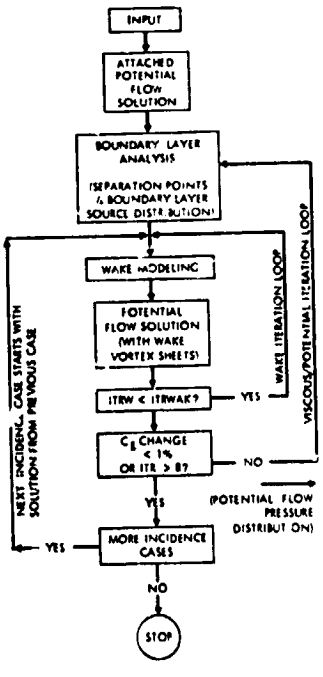

Figure 2.- Calculation procedure.

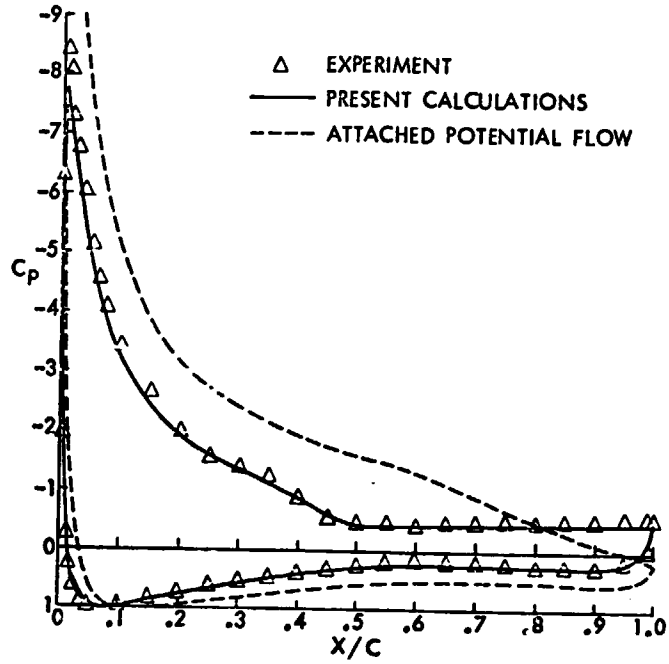

Figure 3.- Comparison of calculated and experimental pressure distributions on a GA(W)-1 airfoil post stall. Re = 6.3×10^6; $\alpha = 20.05°$.

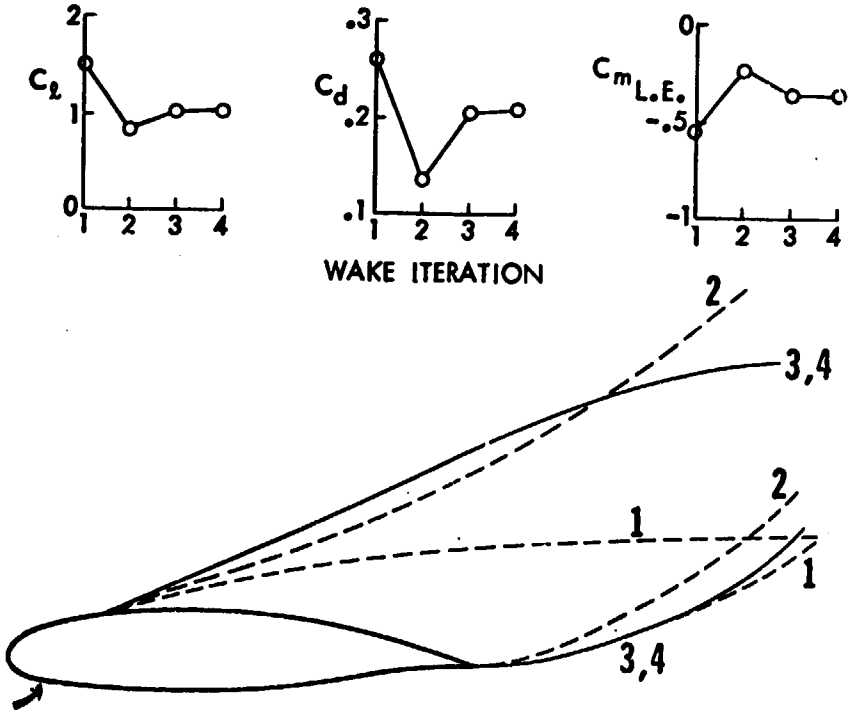

Figure 4.- Typical wake-shape iteration characteristics for an angle of attack beyond the stall.

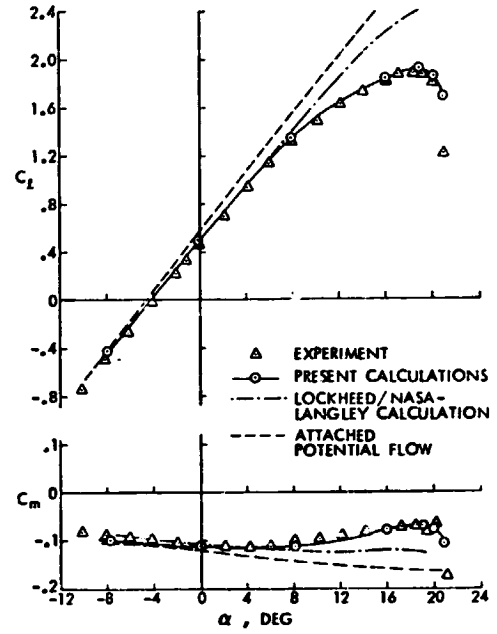

Figure 5.- Comparisons of calculated and experimental lift and pitching-moment characteristics for the GA(W)-1 airfoil. Re = 6.3×10^6.

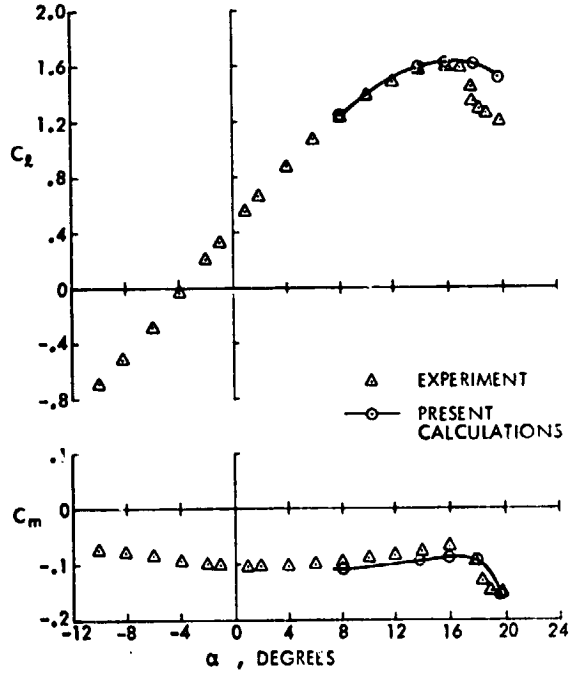

Figure 6.- Comparisons of calculated and experimental lift and pitching-moment characteristics for the GA(W)-1 airfoil. Re = 2.1×10^6.

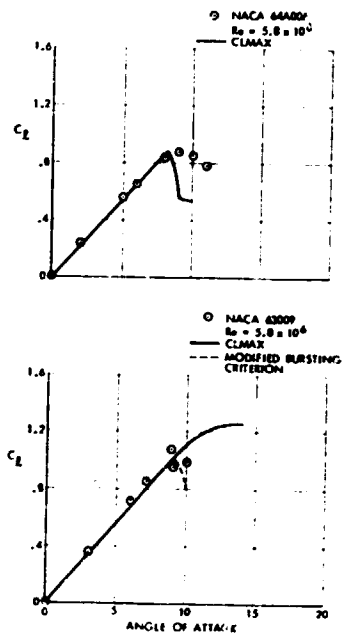

Figure 7.- Comparison of calculated and experimental lift characteristics for NACA 64A006 and 63009 airfoils.

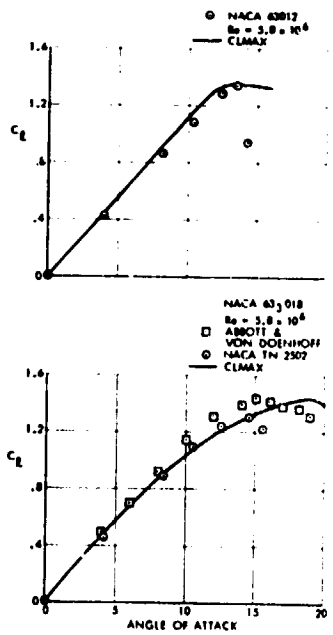

Figure 8.- Comparison of calculated and experimental lift characteristics for NACA 63012 and 63_3018 airfoil sections.

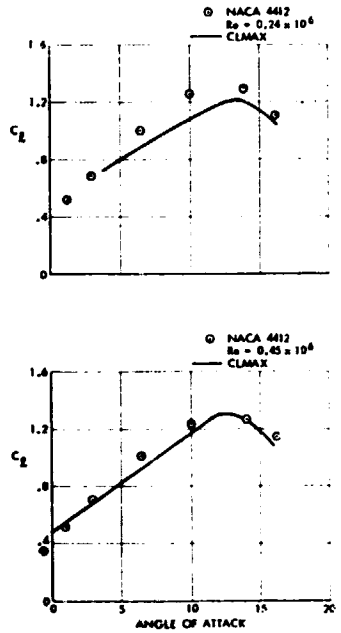

Figure 9.- Comparison of calculated and experimental lift characteristics for an NACA 4412 airfoil. Re = 0.24 × 10^6 and 0.45 × 10^6.

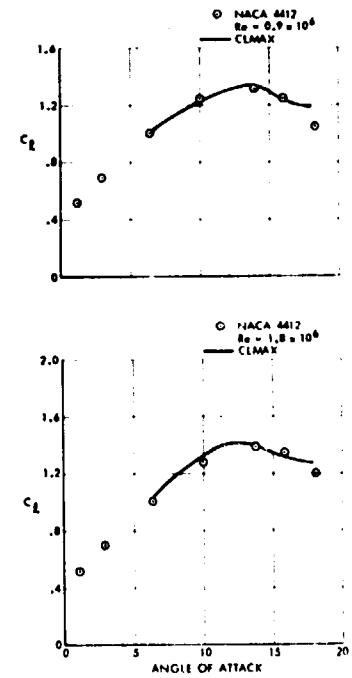

Figure 10.- Comparison of calculated and experimental lift characteristics for an NACA 4412 airfoil. Re = 0.9 × 10^6 and 1.8 × 10^6.

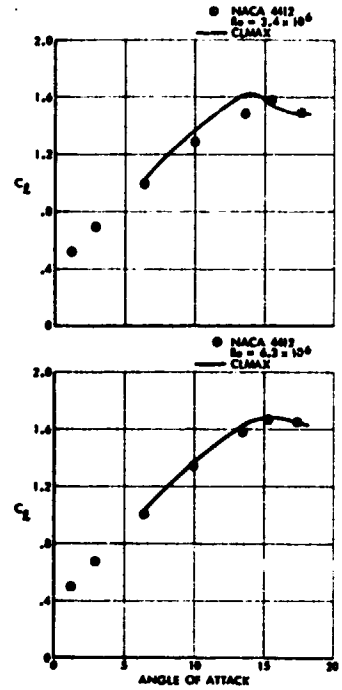

Figure 11.- Comparison of calculated and experimental lift characteristics for an NACA 4412 airfoil. Re = 3.4×10^6 and 6.3×10^6.

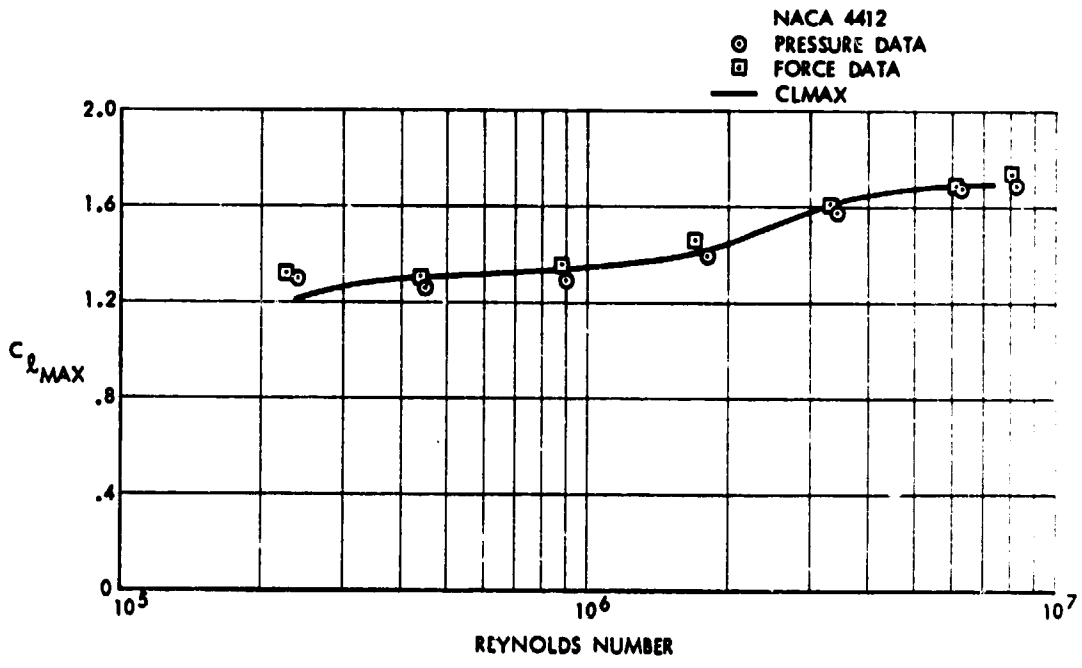

Figure 12.- Comparison of calculated and experimental $C_{\ell_{max}}$ variation with Reynolds number for the NACA 4412 airfoil.

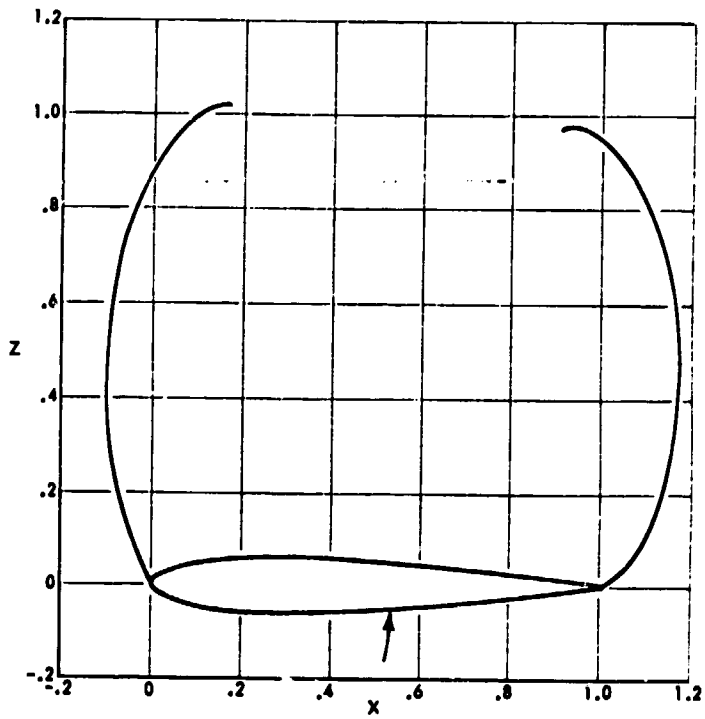

Figure 13.- Calculated wake shape for an NACA 0012 airfoil at 90° incidence after six viscous-potential flow iterations, each with three wake-shape iterations.

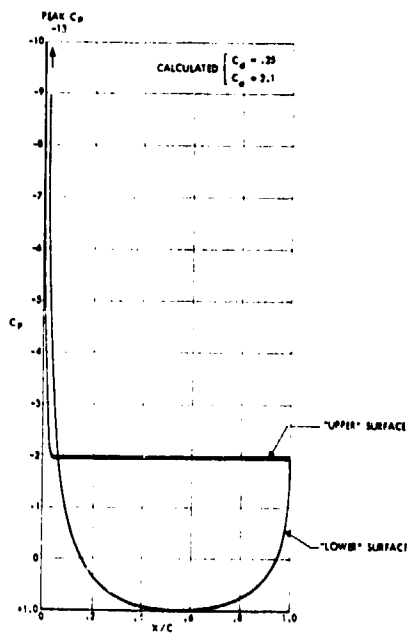

Figure 14.- Calculated pressure distribution on an NACA 0012 airfoil at 90° incidence. Re = 6.0×10^6; Mach number, 0.2.

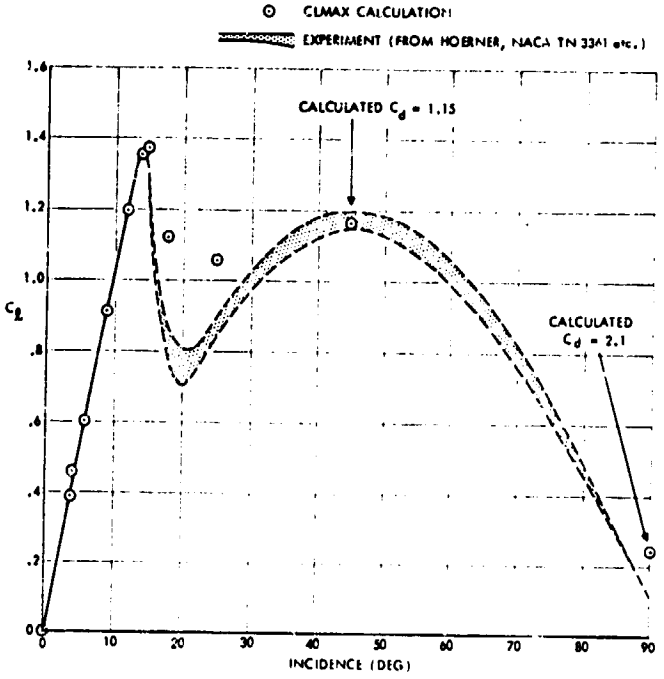

Figure 15.- Comparison of calculated and experimental lift characteristics for an NACA 0012 airfoil. Re = 6.0×10^6; Mach number, 0.2.